



In vitro toxicity of Lithium bis(trifluoromethanesulfonyl)imide (LiTFSI) on Human Renal and Hepatoma Cells

Xing Zhang^a, Mia Sands^a, Mindy Lin^a, Jennifer Guelfo^f, Joseph Irudayaraj^{a,b,c,d,e,*}

^a Department of Bioengineering, University of Illinois, Urbana-Champaign, Urbana, IL 61801, USA

^b Department of Comparative Biosciences, College of Veterinary Medicine, University of Illinois Urbana-Champaign, Urbana, IL 61801, USA

^c Carl Woese Institute for Genomic Biology, University of Illinois, Urbana-Champaign, Urbana, IL 61801, USA

^d Beckman Institute of Technology, University of Illinois, Urbana-Champaign, Urbana, IL 61801, USA

^e Cancer Center at Illinois, University of Illinois, Urbana-Champaign, Urbana, IL 61801, USA

^f Department of Civil, Environmental, and Construction Engineering, Texas Tech University, Lubbock, TX 79409, USA

ARTICLE INFO

Handling Editor: Prof. L.H. Lash

Keywords:

LiTFSI

PFAS

Cytotoxicity

ROS

Apoptosis

Methylation proteins

ABSTRACT

We evaluate the cytotoxicity, intracellular redox conditions, apoptosis, and methylation of *DNMTs/TETs* upon exposure to LiTFSI, a novel Per and Polyfluoroalkyl Substances (PFAS) commonly found in lithium-ion batteries, on human renal carcinoma cells (A498) and hepatoma cells (HepG2). The MTT (3-[4,5-dimethylthiazol-2-yl]-2,5-diphenyl tetrazolium bromide) assay showed both Perfluorooctane sulfonate (PFOS) and Lithium bis(trifluoromethanesulfonyl)imide (LiTFSI) had a dose-dependent effect on A498 and HepG2, with LiTFSI being less toxic. Intracellular redox conditions were assessed with a microplate reader and confocal, which showed a significant decrease in Reactive Oxygen Species (ROS) levels and an increase in Superoxide dismutase (SOD) content in both cells. Exposure to LiTFSI enhanced cell apoptosis, with HepG2 being more susceptible than A498. Quantitative analysis of mRNA expression levels of 19 genes associated with kidney injury, methylation, lipid metabolism and transportation was performed. LiTFSI exposure impacted kidney function by downregulating smooth muscle alpha-actin (*Acta2*) and upregulating transforming growth factor beta 1 (*Tgfb1*), B-cell lymphoma 2-like 1 (*Bcl2l1*), hepatitis A virus cellular receptor 1 (*Harvcr1*), nuclear factor erythroid 2-like 2 (*Nfe2l2*), and hairy and enhancer of split 1 (*Hes1*) expression. LiTFSI exposure also affected the abundance of transcripts associated with DNA methylation by the expression of ten-eleven translocation (*TET*) and DNA methyltransferase (*DNMT*) genes. Furthermore, LiTFSI exposure induced an increase in lipid anabolism and alterations in lipid catabolism in HepG2. Our results provide new insight on the potential role of a new contaminant, LiTFSI in the regulation of oxidative stress, apoptosis and methylation in human renal carcinoma and hepatoma cells.

1. Introduction

Per and Polyfluoroalkyl Substances (PFAS) are fluorinated substances that contain at least one fully fluorinated methyl or methylene carbon atom [13]. PFAS usually contains a hydrophobic and oleophobic carbon chain structure and a hydrophilic functional group [50]. The structure of PFAS encompasses carbon-fluorine (C-F) bonds which has a high bond energy and strong polarity [23]. The amphiphilicity and C-F bonds contribute to the stability, surface activity, hydrophobic, and oleophobic properties of PFAS. PFAS have been widely used in the production of various industrial and household products, such as the coatings on non-stick pans, hydrophobic and oleophobic coatings, foam fire extinguishing agents, and surfactants [29]. Due to the highly stable

C-F bonds, PFAS are recalcitrant, resulting in their lasting persistence in the environment and the human body [14].

The widespread use of PFAS has raised concerns on the toxic effects and human health risks. Numerous studies have shown that PFAS are widely prevalent in the environmental media and organisms including air [8], sludge [21], surface water [20], soil [2], and even polar ice sheets [26], wild animals [22], and humans [48]. After entering the human body, PFAS chemicals accumulate in organs via the blood circulatory system, causing damage and endocrine disruption [1,17].

Our specific focus is the in vitro toxicity of LiTFSI (CAS No. 90076–65–6), also known as lithium bis(trifluoromethanesulfonyl) imide, $\text{LiNH}(\text{CF}_3\text{SO}_2)_2$, a lithium salt with a weak coordination anion [28]. Due to its superior electrochemical stability and conductivity,

* Corresponding author at: Department of Bioengineering, University of Illinois, Urbana-Champaign, Urbana, IL 61801, USA

E-mail address: jirudaya@illinois.edu (J. Irudayaraj).

<https://doi.org/10.1016/j.toxrep.2024.02.008>

Received 5 December 2023; Received in revised form 11 February 2024; Accepted 28 February 2024

Available online 1 March 2024

2214-7500/© 2024 The Authors. Published by Elsevier B.V. This is an open access article under the CC BY-NC-ND license (<http://creativecommons.org/licenses/by-nc-nd/4.0/>).

LiTFSI is a popular choice as a composite polymer electrolyte material, often utilized in lithium-ion batteries and organic electrolyte lithium salts [49]. LiTFSI is considered to be a type of PFAS due to its similarity in molecular structure [18]. It contains a perfluoroalkyl chain and shares many parallels with other PFAS and is also highly stable and persistent in the environment. Despite its prolonged and widespread use in the energy sectors, the toxic effects of LiTFSI have yet to be studied; the potential adverse effects on human health and the environment are largely unknown. It is believed that it may share some of the same properties and potential risks as other PFAS. Our work investigates the potential toxic effects of LiTFSI in relation to the kidney and liver, *in vitro*.

Livers and kidneys are some of the most common organs for contaminant accumulation. PFAS exposure induced hepatomegaly [45], chronic kidney disease (CKD) [30] and cancer in mice. PFAS is also known to induce oxidative stress, which can lead to cell death and tissue damage in severe cases [33,34,47]. Exposure to certain PFAS has been associated with liver damage [11], including inflammation, hepatocyte necrosis, and liver tumors. Additionally, PFAS exposure has been shown to increase liver weight, alter liver enzymes and lipid metabolism, and induce oxidative stress [38]. A study of individuals exposed to PFAS through contaminated drinking water found a positive association between PFAS exposure and increased liver enzymes [39]. Exposure to PFAS has been linked to decreased kidney function, such as decreased glomerular filtration rate (GFR) [42] and increased albuminuria [24], which are signs of kidney disease. Given these findings, we hypothesize that LiTFSI may disrupt liver and kidney function and potentially exacerbate liver and kidney disease. To investigate this, we will utilize HepG2 cells, derived from human hepatocellular carcinoma, and A498 cells, derived from human renal cell carcinoma, as *in vitro* models to examine LiTFSI-induced hepatotoxicity and nephrotoxicity. Both A498 and HepG2 cell lines have been extensively characterized and widely used in toxicological studies [19,3,32,44].

We will investigate the short-term toxicity of LiTFSI on cell viability, reactive oxygen species (ROS) and superoxide dismutase (SOD) levels, apoptosis, cell cycle, and gene expression related to methylation. We expect our foundational work to provide the basis for future research on the use and mitigation of PFAS compounds such as LiTFSI.

2. Materials and Methods

2.1. Chemicals and test reagents

The lithium salt form of LiTFSI, Lithium bis(trifluoromethanesulfonyl)imide (CAS No. 90076–65–6) 99.99% grade was purchased from Sigma-Aldrich Corporation (St. Louis, MO, USA). Perfluorooctane sulfonate (PFOS) was purchased from SynQuest Labs (Alachua, FL, USA). LiTFSI and PFOS were dissolved in dimethyl sulfoxide (DMSO; CAS No. D8418) from Sigma-Aldrich to obtain a stock solution of 0.1 M. Fig. 1

2.2. Cell culture

The HepG2 (ATCC HB-8065) and A498 (ATCC HTB-44) cell lines were obtained from the Cancer Center at Illinois, University of Illinois Urbana-Champaign. HepG2 cells were cultured in Dulbecco's Modified Eagle's Medium (ATCC 30–2002; Manassas, VA, USA) supplemented with 10% fetal bovine serum (FBS, Gibco™ 10082147; Thermo Fisher Scientific; Waltham, MA, USA) and 1% Penicillin Streptomycin Solution (REF 30–002-Cl; Corning, NY, USA). A498 was cultured in Eagle's Minimum Essential Medium (ATCC 30–2003; Manassas, VA, USA) supplemented with 10% FBS and 1% Penicillin Streptomycin Solution. Culture conditions for all cells were at 37°C in a humidified 5% CO₂ atmosphere. All experiments were performed independently in triplicate.

2.3. 3-[4,5-dimethylthiazol-2-yl]-2,5 diphenyl tetrazolium bromide (MTT) assay

Cell growth and proliferation assay at 0, 50, 100, 150, 200 or 250 µM of LiTFSI and PFOS were measured with the MTT assay kit (Invitrogen, Cat. No. M6494). Cells were plated into a 96-well microplate (Corning Incorporated, New York, USA) and incubated at 37 °C in 5% CO₂. Each data point represents measurement from three replicate wells. The cells were cultured to 30–40% confluence before corresponding treatments and cultured for another 24 h or 48 h to reach a final confluence of 50–90%. After exposure to chemicals, 10 µl of MTT reagent was added to each well with 90 µl of serum-free medium and incubated for another 4 h at 37 °C. MTT reagent was then added to the medium to stop the reaction and the absorbance, at 570 nm, was measured using a microplate reader (Synergy HT, BioTek; Winooski, VT, USA).

2.4. ROS/Superoxide detection

The production of ROS and superoxide were measured in A498, and HepG2 cells by ROS/Superoxide Detection Assay Kit (Cell-based) (ab139476; Abcam; Waltham, MA, USA). Cells were loaded with the ROS/Superoxide Detection Mix at 37°C for 30–60 min in the dark. For confocal measurements the detection mixture was removed from glass slides and cells were washed gently with wash buffer and observed under confocal microscopy with fluorescein (Ex/Em = 490/525 nm). For microplate reading, cells were washed and incubated with chemicals in a 96-well plate for 4 h and fluorescence was measured with standard fluorescein (Ex/Em=488 nm/520 nm) and rhodamine (Ex/Em=550 nm/610 nm) filter sets at endpoint mode.

2.5. Apoptosis assay

To investigate the effects of LiTFSI and PFOS on apoptosis, A498 and HepG2 cells were cultured with chemicals in 6-well plates. After 24 h, plates were harvested and incubated. A TACS® 2 TdT-Fluor *In Situ* Apoptosis Detection Kit (4812–30-K, Minneapolis, MN, USA) was used

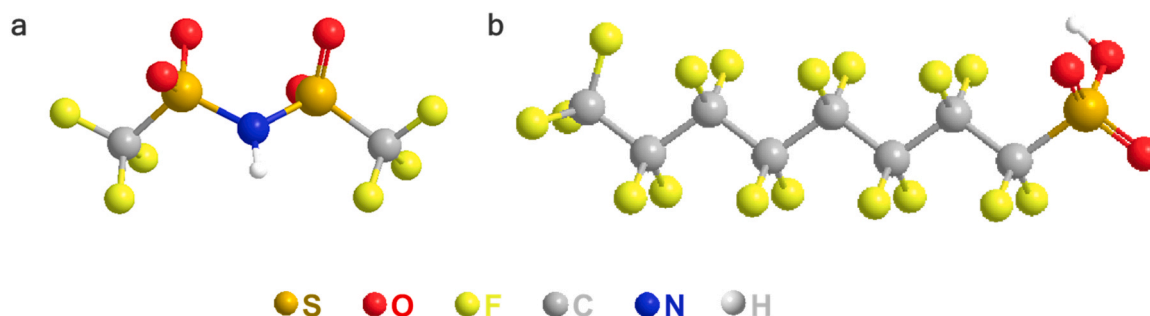


Fig. 1. Chemical structure of (a) LiTFSI and (b) PFOS.

per manufacturer's instruction to determine the level of cell apoptosis. Apoptotic cells were analyzed using a BD LSR Fortessa CMtO Analyzer equipped with HTS (High Throughput Sampler) flow cytometer.

2.6. Cell cycle assay

Cells in the logarithmic growth phase were incubated with serum-free medium for 6 h to arrest all cells at G0/G1 phase, followed by exposure to different concentrations of LiTFSI. After 48 h, the cells were fixed with pre-cooled absolute ethanol, resuspended in RNaseA, and stained with propidium iodide (PI). Cell cycle was analyzed using a BD LSR Fortessa CMtO Analyzer equipped with a High Throughput Screening (HTS) flow cytometer.

2.7. Gene expression analysis

Total RNA was isolated using GeneJET RNA Purification Kit (K0731, Thermo Fisher Scientific; Waltham, MA, USA) and DNA-free™ DNA Removal Kit (AM1906, Thermo Fisher Scientific; Waltham, MA, USA) was used to remove the genomic DNA. The quantity and quality of extracted RNA were tested with NanoDrop One. cDNA synthesis was performed by high-capacity cDNA Reverse Transcription Kit (Applied Biosystems REF 4368814; Waltham, MA, USA). Analysis of mRNA was performed by Quantitative reverse transcription polymerase chain reaction (qRT-PCR) using SYBR Green PCR Master Mix reagents (Applied Biosystems REF 4367659; Waltham, MA, USA) according to manufacturer's specifications, with a Step One Plus RealTime PCR System (Applied Biosystems, Waltham, MA, USA). Relative quantification was obtained by normalization to GAPDH expression levels. Reactions were run in triplicate. The expression levels of mRNAs were determined by the $2^{-\Delta\Delta Ct}$ method for relative quantification of gene expression. All primer sequences were listed in Table S1.

2.8. Statistical analysis

The data obtained was analyzed using SPSS software, while the

graphical illustrations were generated using GraphPad Prism 9 Software. The data was expressed as the mean \pm standard error of the mean (SEM), MTT assay, ROS/Superoxide detection, Apoptosis assay, Cell cycle assay, and Gene expression analysis are all three independent biological experiments, and each experiment has three technical replicates. And the statistical significance of the difference between the two experimental groups was determined using Student's t-test. We used analysis of variance (ANOVA) to assess whether there are any statistically significant differences among the means of multiple treatment groups. A significance level of $P < 0.05$ was considered statistically significant.

3. Results

3.1. Cytotoxicity assessment

The cytotoxic effect of LiTFSI on human carcinoma renal cell lines, A498 and further on human hepatoma cells HepG2 were first assayed using the MTT reagent. Well-known PFOS was used as a positive control to compare the cytotoxicity behavior of the two compounds. Based on a previous study with PFOS at 300 μM (resulting in 50% cell death) and 24 h of exposure [16], we chose a concentration of up to 250 μM to maintain cell viability after 48 h of treatment. Two cell lines were incubated with different concentrations (50, 100, 150, 200 or 250 μM) of the chemicals for 24 h and 48 h.

Cell viability decreased upon treatment with LiTFSI and PFOS in a dose-dependent manner (Fig. 2). In A498 cells, the concentration of the two chemicals at 100 μM had no effect on cell viability. The 24 h and 48 h cell viability of LiTFSI treatment at 150 μM decreased to 88% and 82%, while the PFOS treatment was 72% and 67% respectively. HepG2 cells were significantly more sensitive to LiTFSI and positive control. HepG2 cells exposed to PFOS exhibited 60% and 51% more cell death than LiTFSI at 150 μM . The viability of two cells exposed to DMSO was not significantly different from the untreated control group, hence only the blank was used as the negative control.

The concentration of DMSO used in all treatments and controls was

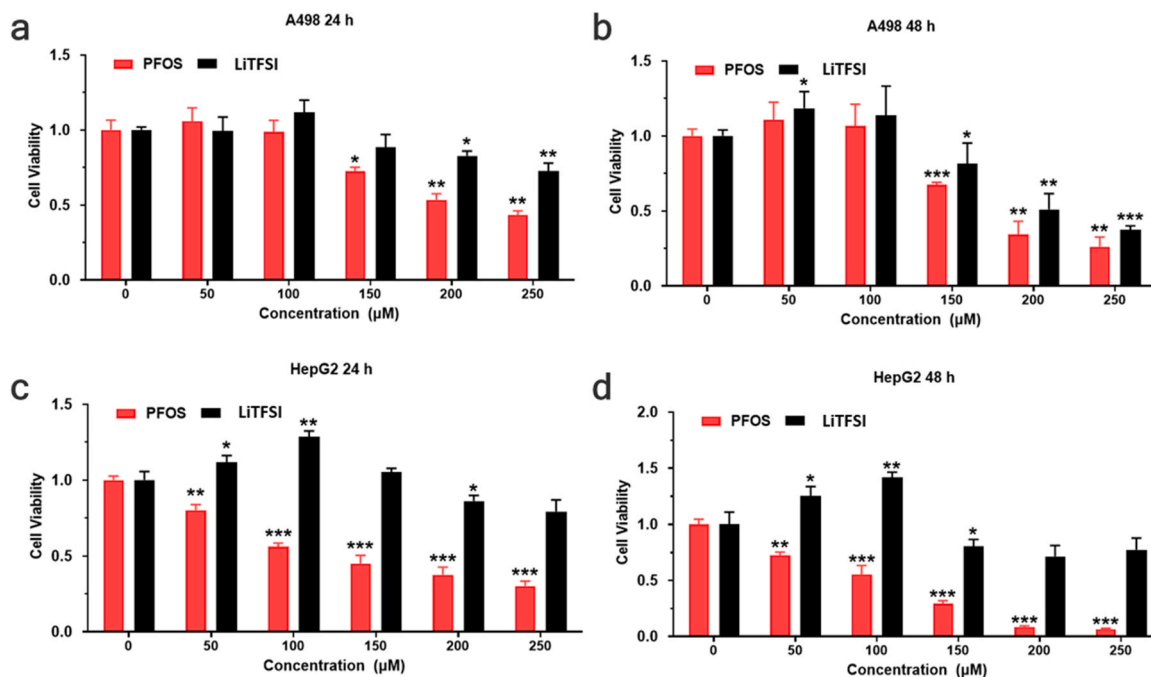


Fig. 2. Cytotoxicity assessment of PFOS and LiTFSI in A498 and HepG2 cells. (a) and (b) show the viability evaluation of A498 cells exposed to PFOS and LiTFSI for 24 and 48 hours, respectively, using the MTT assay. Similarly, (c) and (d) depict the viability of HepG2 cells exposed to PFOS and LiTFSI for 24 and 48 hours, respectively, also assessed via the MTT assay. Each experiment was conducted in triplicate. Statistical significance was determined using the symbol * $p < 0.05$ compared with untreated controls (NC).

kept below 0.4% v/v to minimize its potential influence on cell response. Figure S1 demonstrated that a concentration of 1.6% v/v DMSO had negligible effects when evaluated with MTT assay.

Our data collectively suggests that LiTFSI and PFOS have cytotoxicity on human carcinoma renal cells and hepatoma cells. LiTFSI was less toxic and had higher cell survival after exposure. HepG2 cells were more sensitive to both chemicals.

3.2. Intracellular redox conditions and DNA damage

The redox effects of LiTFSI on A498 and HepG2 were assayed using the microplate (Fig. 3a, Figure S8) and confocal imaging (Fig. 3b). After exposure to A498 and HepG2 cells, the stimulation of ROS and SOD production by LiTFSI was measured. The results of the microplate assay showed a marked reduction in ROS levels in A498 cells. Upon exposure to a concentration of 200 μM of LiTFSI, a significant decrease in ROS levels (by 29%) was noted. Additionally, a simultaneous increase (54%) in SOD content was observed at a concentration of 250 μM , demonstrating a dose-dependent effect. Confocal microscopy results were consistent with the microplate assay, demonstrating an enhancement of red fluorescence, representing an increase in SOD content. The results of HepG2 revealed a phenomenon that was similar to that observed in A498 cells. At a concentration of 250 μM , a decrease in ROS levels by up to 6% was noted while a corresponding increase in SOD content was 29% compared to the control group. To further confirm that intracellular ROS is reduced after exposure to LiTFSI, two significant treatment concentrations (100 μM and 200 μM) were selected and a comprehensive time-course analysis (0 h, 2 h, 4 h, 6 h, 8 h, 12 h and 24 h) was conducted to monitor ROS generation (Figure S9). During the time course of 100 μM LiTFSI treatment in both A498 and HepG2 cells, a significant reduction in ROS generation after 4 h of exposure was observed. Figure S9 shown a similar trend during the time course of 200 μM LiTFSI treatment in both cell lines, with a significant reduction in ROS generation after 2–4 h of exposure.

To better study the effect of LiTFSI on DNA damage, Comet Assay was used in both A498 and HepG2 cells (Figure S10). Following a 24-hour treatment with various concentrations of LiTFSI (ranging from 0 μM to 250 μM), as shown in Figure S10, both cell lines exhibited a dose-dependent increase in DNA damage, as evidenced by the visualization of comet tail lengths. Negative control of A498 and HepG2 cells exhibited minimal DNA damage. Specifically, A498 cells showed significant damage even with exposure to just 50 μM of LiTFSI, while HepG2 cells displayed significant damage after exposure to 100 μM

LiTFSI. These findings confirm that LiTFSI treatment induces DNA damage, with the level of damage becoming more pronounced as the concentration of LiTFSI increases in both cell lines.

These findings provide insight into the potential role of LiTFSI in regulating cellular oxidative stress and inducing DNA damage in the two cell lines. Further investigation and analysis are necessary to fully understand the underlying mechanisms and implications of these findings.

3.3. Cell apoptosis

Cell apoptosis was evaluated by flow cytometry after exposure to LiTFSI for 24 h. Results showed a remarkable increase in the percentage of apoptotic cells in the two cells ($p < 0.05$, Fig. 4a, b, c, and d). HepG2 cells exhibited a higher susceptibility to apoptosis compared to A498 cells. At a concentration of 250 μM , the apoptosis rate of A498 cells was 8.1%, representing a 146% increase compared to the control group. Meanwhile, the apoptosis rate of HepG2 cells was 17.02% under the same conditions.

Due to the influence of LiTFSI on cell viability and apoptosis, several genes related to apoptosis and proliferation were evaluated. Results showed that the expression of *BCL2*-associated X (*BAX*) in A498 cells initially increased and then decreased, reaching the highest expression at a concentration of 150 μM LiTFSI. This expression was 1.4 times greater than the control group. Results revealed a decrease in the expression of *BAX* in HepG2 cells following exposure to LiTFSI. As the dosage increased, the expression of *BAX* showed a significant dose-dependent decrease. To further determine the effect of LiTFSI on apoptosis, we examined the ratio of *Bax/Bcl-2* which provides insight into the balance between pro-apoptotic and anti-apoptotic factors within cells. In both cell lines, the *BAX/Bcl2* ratio became larger after exposure to LiTFSI. A higher *Bax/Bcl-2* ratio generally indicates a shift toward pro-apoptotic signaling, which was more significant in HepG2 cells.

Additionally, the expression of the four genes related to cell proliferation, Cyclin-dependent kinase inhibitor 1 A (*CDKN1A*), Cyclin-dependent kinase 4 (*CDK4*), Ribosomal protein S6 (*RPS6*), *KIT* ligand (*KITLG*), were analyzed. *CDKN1A* increased significantly at higher levels of LiTFSI exposure in both the cell lines, while *CDK4* exhibited a remarkable decrease. In A498 cells, there was no significant change in the expression of *RPS6* after exposure to LiTFSI. Conversely, in HepG2 cells, a significant down-regulation of *RPS6* was observed at high concentrations of LiTFSI. The expression of *KITLG* decreased at most concentrations in A498. *KITLG* expression decreased at 150 μM of LiTFSI

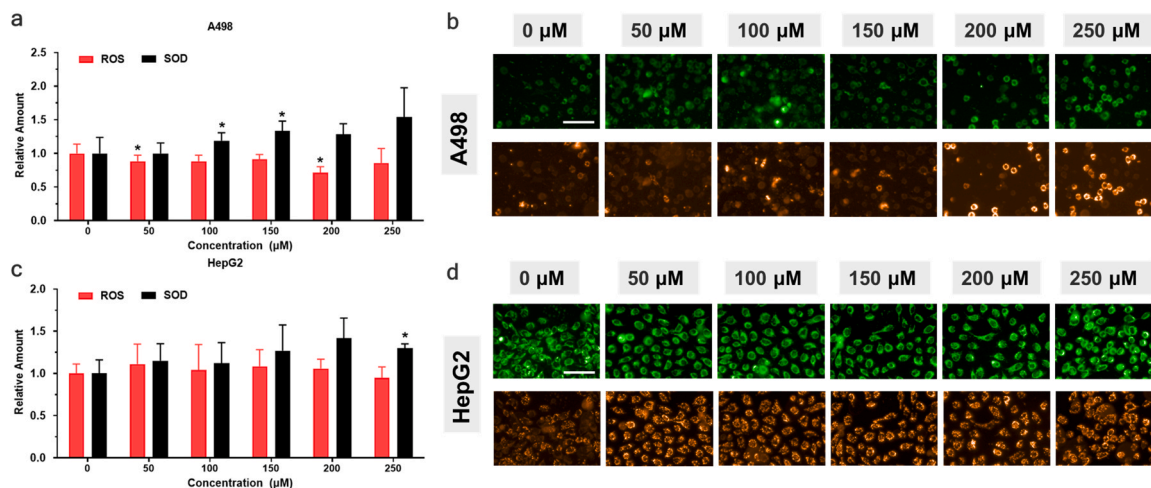


Fig. 3. Intracellular ROS and SOD activity in A498 and HepG2 cells after 24 h exposure to different concentration of LiTFSI. (a) and (c) depict the relative amount of ROS and SOD, respectively, measured through microplate readings, while (b) and (d) illustrate the observed intensity of fluorescein under microscopy. Data represent the mean \pm SD of three independent experiments, with statistical significance denoted by * $p < 0.05$ compared with untreated controls (NC).

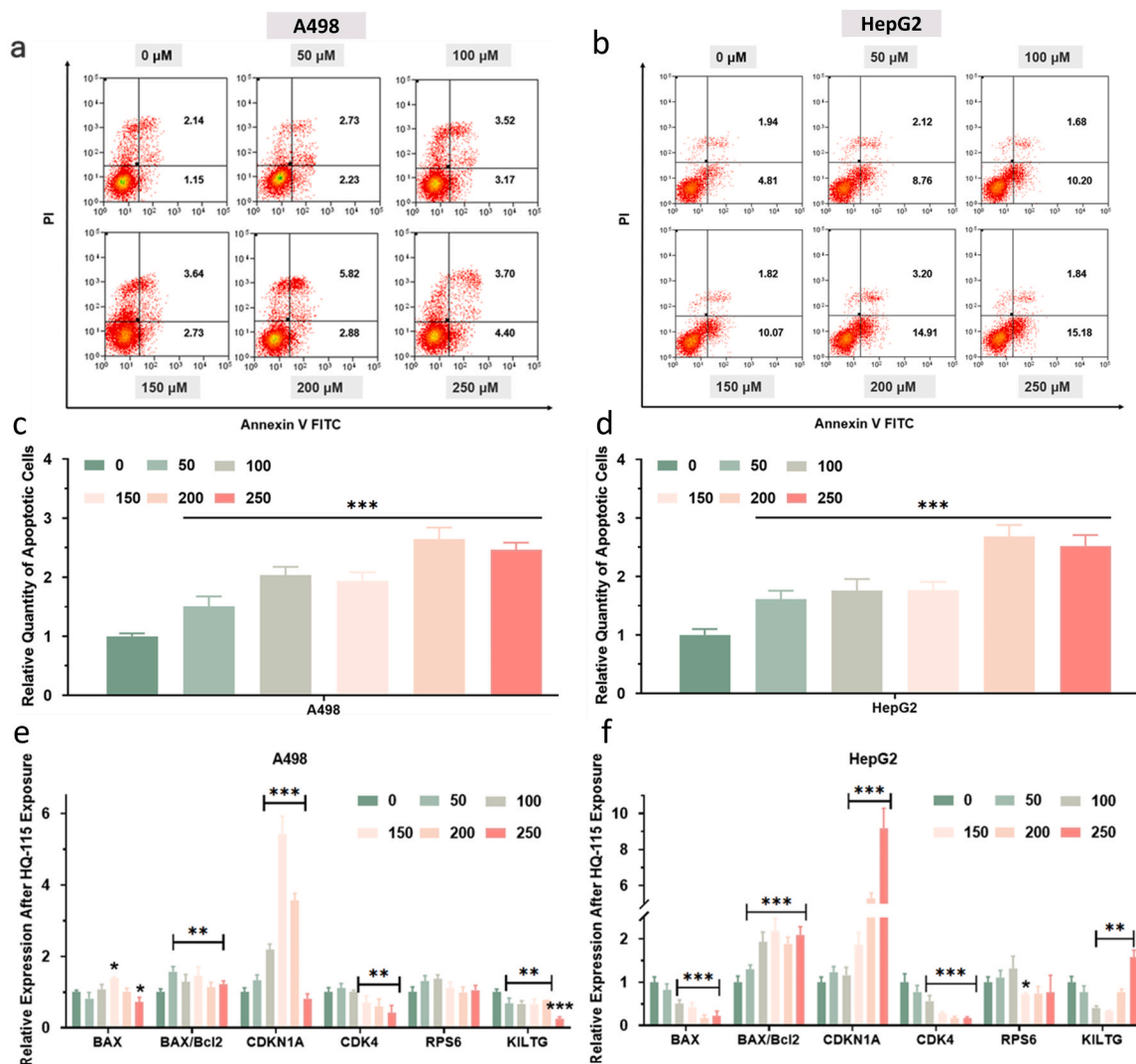


Fig. 4. Cell apoptosis in A498 and HepG2 cells following 24-hour exposure to LiTFSI. (a) and (b) display the apoptosis distributions of A498 and HepG2 cells, respectively, detected by flow cytometry after exposure to LiTFSI for 24 hours. (c) and (d) show the relative quantity of apoptotic cells in the treated A498 and HepG2 cells, respectively. (e) and (f) present the relative expression of apoptosis-related genes in A498 cells and HepG2 cells after 48 hours of exposure to LiTFSI. Each experiment was conducted in triplicate. Statistical significance is denoted by * $p < 0.05$ compared with untreated controls (NC).

treatment and increased at all higher concentrations in HepG2. We conducted further evaluation of DNA damage using the comet assay, which revealed an increase in DNA damage corresponding to higher dosages of LiTFSI (refer to Figure S9).

3.4. Dysregulation of cell cycle

Dysregulation of cell proliferation due to cell cycle abnormalities is a hallmark of tumorigenesis. To investigate whether LiTFSI influences cell proliferation by regulating cell cycle progression, we evaluated the expression of cell cycle genes in A498 and HepG2 cells (Fig. 5a, Fig. 5b, Figure S2 and Figure S3). Our results revealed that LiTFSI induced cell cycle arrest in the S phase in HepG2 cells, the proportion of cells in S phase increased by 67% at 150 μM LiTFSI compared to control. However, in A498 cells, LiTFSI did not affect cell cycle progression.

The expression of cell cycle-related genes cyclin A2 (*Ccna2*), cyclin E1 (*Ccne1*) and cyclin B1 (*Ccnb1*) were examined by qPCR to provide insights on the molecular mechanisms underlying the effect of LiTFSI on cell cycle progression. In our study, we observed differential regulation of *Ccna2*, *Ccne1*, and *Ccnb1* in A498 and HepG2 cells upon exposure to LiTFSI. In the A498 cells, the expression of *Ccna2*, *Ccne1*, and *Ccnb1*

genes exhibited a significant upregulation at 150 μM of LiTFSI treatment, followed by downregulation at higher concentrations. In contrast, all three genes showed significant downregulation in HepG2 cells after treatment.

These findings suggest that the effects of LiTFSI on cell cycle progression may involve the selective modulation of specific cell cycle regulatory genes and is potentially cell type dependent.

3.5. Effect on kidney damage and methylation genes

The carcinogenic potential of PFAS in humans has been reported in previous studies [15,36,40]. Hence, the effect of PFAS on key genes associated with kidney injury, lipid metabolism and transportation as well as methylation was examined. A total of 19 mRNA expression levels were quantified and analyzed in this study.

The expression of genes associated with kidney injury and their response to LiTFSI exposure was investigated (Fig. 6a, and Figure S4). Six genes were selected for evaluation and mRNA expression was performed on A498 cells. Among the genes studied, *Acta2* expression was significant decreased at LiTFSI doses of 100 μM and higher. *Tgfb1* and *Bcl2l1* exhibited a significant increase in gene expression only at a

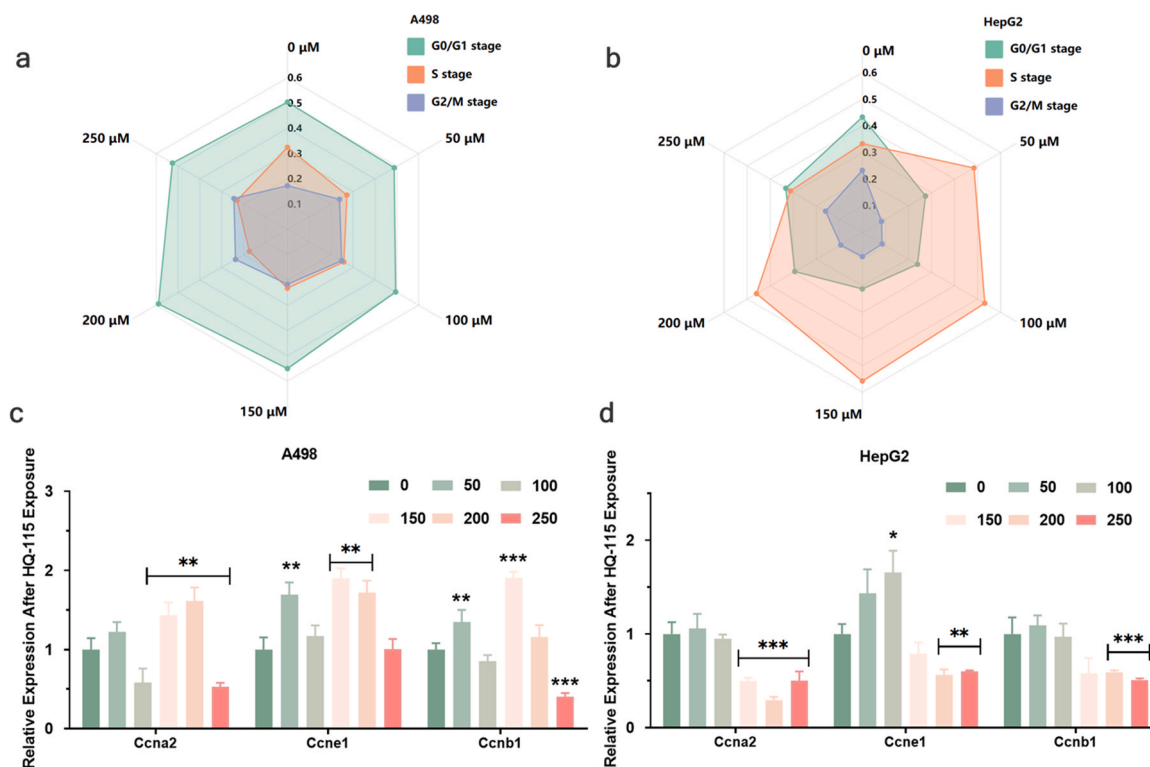


Fig. 5. Cell cycle analysis of A498 and HepG2 cells following exposure to LiTFSI. (a) and (b) depict the cell cycle distributions of A498 and HepG2 cells, respectively, detected by flow cytometry after 48 hours of LiTFSI exposure. (c) and (d) show the relative expression of cell cycle-related genes in A498 and HepG2 cells, respectively, also after 48 hours of LiTFSI exposure. Each experiment was conducted in triplicate. Statistical significance is indicated by * $p < 0.05$ compared with untreated controls (NC).

concentration of 150 μM , which was twice the control level, and insignificant changes were observed at other concentrations. In contrast, *Harvcr1*, *Nfe2l2*, and *Hes1* displayed significant increase expression at higher concentrations ($>200 \mu\text{M}$). The results provide evidence of a dose-dependent response of these genes to LiTFSI exposure and suggest that LiTFSI may have an impact on kidney function.

The methylation changes were investigated by assessing the relative gene expression profiles of ten-eleven translocation (*TET*) and DNA methyltransferase (*DNMT*) (*TET1*, *TET2*, *TET3*, *DNMT1*, *DNMT3A*, and *DNMT3B*), which are involved in the regulation of DNA methylation via *TET* methylcytosine dioxygenase and DNA methyltransferase enzymes. The expression of these genes was assessed in cells treated with different concentrations of LiTFSI (Figure S5). Our results revealed that with an increase in concentration of LiTFSI, the expression of *TET* family of genes exhibited an initial increase and subsequent decrease, with the highest expression observed at concentrations between 150 μM and 200 μM , which was more than 3 times higher than the control group. However, the expression of *DNMT1* was not significantly affected, while *DNMT3A* and *DNMT3B* were significantly downregulated, both of which were less than half the control group. These findings suggest that LiTFSI may play a role in regulating the abundance of transcripts associated with DNA methylation through its effects on the expression of *TET* and *DNMT* genes.

3.6. Effect on lipid metabolism, transportation and methylation genes

Among the evaluated genes (Fig. 6b), the expression of Acyl-CoA dehydrogenase family member 11 (*ACAD11*) and Acyl-CoA dehydrogenase medium chain (*ACADM*), which are involved in β -oxidation of fatty acids, showed a biphasic response upon exposure to LiTFSI, with an initial increase followed by a decrease. Conversely, the expression of Acyl-CoA synthetase long-chain family member 1 (*ACSL1*), a gene related to lipid synthesis significantly increased in a dose-dependent

manner. *ACSL1* expression increased ~ 6.5 -fold upon exposure to 200 μM LiTFSI (Figure S5). Acyl CoA Oxidase 2 (*ACOX2*), encoding an enzyme involved in fatty acid degradation in peroxisomes, exhibited a significant reduction in its expression upon treatment with LiTFSI. Our results showed that exposure to LiTFSI at a concentration of 200 μM resulted in a significant increase in the expression of 3-hydroxy-3-methylglutaryl-CoA reductase (*HMGCR*), which encodes the rate-limiting enzyme in cholesterol synthesis. The fold change was approximately 5 times greater than the control group (Figure S6). Furthermore, we observed a clear modulation of transport genes related to lipid metabolism.

The expressions of *TET* and *DNMT* family were assessed in cells exposed to different concentrations of LiTFSI (Figure S7). The expression of *TET1* and *TET3* displayed a downward trend (Less than 0.5 times) with increasing LiTFSI dose, while *TET2* expression was increased at higher concentrations of LiTFSI (250 μM). Notably, the expression of all three *DNMT* genes showed a significant dose-response change.

The expression levels of the histone methyltransferase Euchromatic histone-lysine N-methyltransferase 2 (*Ehmt2*) and the lysine-specific histone demethylases *Kdm1a*, *Kdm4a*, *Kdm4b*, *Kdm4c*, and *Kdm4d* were assessed across all treatment groups. At all treatment levels, there was a significant increase in the expression of demethylases genes in A498 cells. However, for HepG2 cells, the increase in these genes was observed only at higher doses.

These results suggest that LiTFSI exposure could induce an increase in lipid anabolism and alterations in lipid catabolism in HepG2 cells. Our results shed light on the potential involvement of *TET* methylcytosine dioxygenases and DNA methyltransferases based on the observed methylation changes following exposure to LiTFSI in HepG2.

4. Discussion

Per- and polyfluoroalkyl substances (PFAS) have been noted to

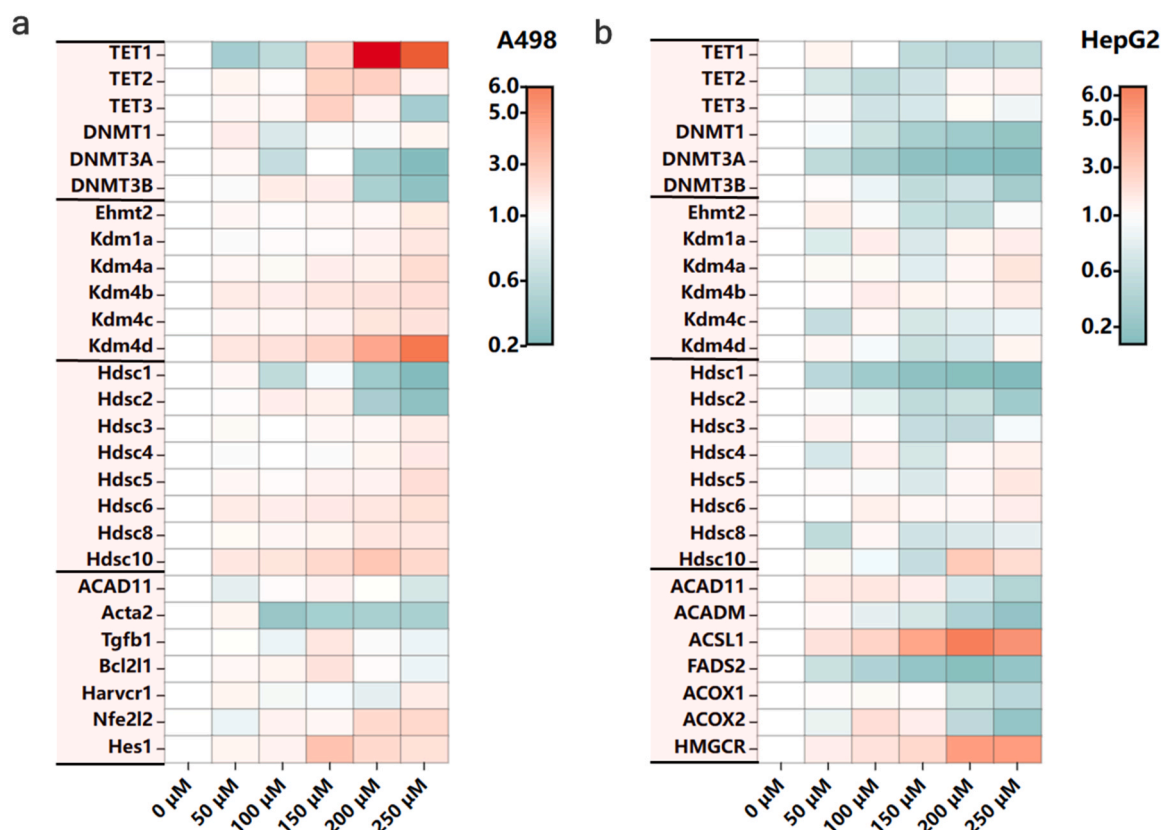


Fig. 6. Gene expression analysis after 24 h LiTFSI exposure in A498 and HepG2 cell lines (a) Effect of LiTFSI on the expression of DNA methylation, histone methylation, histone acetylation and kidney damage related genes in A498. (b) Effect of LiTFSI on the expression of DNA methylation, histone methylation, histone acetylation and lipid metabolism, transportation related genes in HepG2. Experiments were repeated three times. * $p < 0.05$ compared with untreated controls(NC).

impart adverse effects on liver and kidney function [13,43]. LiTFSI is designed for various industrial and commercial applications, including backup power systems, renewable energy storage systems, electric vehicles, and other high energy demanding applications [37]. Despite the widespread use of LiTFSI in lithium-ion batteries and electronic devices, its toxicity has not been evaluated. Understanding the toxicity and persistence of LiTFSI will help inform future risk assessments and regulatory actions to protect human and environmental health. In the present study, we aim to elucidate the potential health risks of LiTFSI.

Compared with our previous study, LiTFSI was less cytotoxic than PFOA, PFOS, or GenX (ammonium salt of hexafluoropropylene oxide dimer acid) [45,46]. In our manuscript, low concentrations (50 μM and 100 μM) of LiTFSI can increase cell viability, which is a Hormesis Effect. Low concentrations of PFPrA (Perfluoropropionic acid), PFBA (Perfluorobutanoic acid), PFDA (Perfluorodecanoic acid) could increase cell viability [4], possibly due to PFAS could trigger adaptive responses or cellular repair mechanisms. Our manuscript also shows that LiTFSI reduces intracellular ROS content, which can be beneficial for cell health and viability. The observed decrease in cell viability and increase in SOD production in both A498 and HepG2 cells following exposure to LiTFSI are consistent with previous studies which show that exposure to PFAS can induce oxidative stress and DNA damage in human cells [12,34]. However, the response of the two cell types to the oxidative stress is different, as indicated by their SOD expression levels. The upregulation of SOD expression in HepG2 cells indicates that these cells may mount an adaptive response to the oxidative stress induced by LiTFSI exposure. This increase in SOD expression allows the cells to effectively scavenge ROS and protect against oxidative damage which can lead to an increase in cell survival [41]. However, the downregulation of SOD expression in A498 cells suggests that these cells may not be able to counteract the oxidative stress effectively. This decrease in SOD expression leads to an

accumulation of ROS in the cells, which can cause oxidative damage and ultimately decrease cell viability. Therefore, the differential regulation of SOD expression in HepG2 and A498 cells suggests that HepG2 cells can better cope with oxidative stress upon exposure to LiTFSI, while A498 cells may be more susceptible to the negative effects of oxidative stress.

The induction of apoptosis in both cell lines is similar to previous studies which show that PFAS can induce programmable cell death [6]. Our findings also reveal that LiTFSI may modulate the expression of genes involved in the intrinsic and extrinsic apoptotic pathways in a cell type-specific manner. The study also evaluated the expression of genes related to apoptosis and proliferation in both cell lines. The expression of *BAX* [5], a pro-apoptotic gene, was found to increase initially in A498 cells but decrease in a dose-dependent manner in HepG2 cells. In addition, the expression of *RPS6* is different in the two cell lines studied. *RPS6* may be involved in adipogenesis and promote the development of human hepatocellular carcinoma [7]. The expression of *KITLG*, a gene involved in cell growth, decreased in A498 cells but increased in HepG2 cells. Taken together, our findings suggest that LiTFSI may modulate the expression of genes involved in apoptosis and proliferation. This could be due to differences in the expression of specific genes or proteins in the two cell types, or to differences in the way that LiTFSI interacts with these genes or proteins.

The modulation of cell cycle progression by LiTFSI is another important finding of this study. Previous research has indicated that PFOS, PFBS (Perfluorobutane Sulfonic Acid) and PFBA (Perfluorobutanoic acid) could arrest cells in the G0 and G1 phases and decrease the number of cells in the S phase on bottlenose dolphin (*Tursiops truncatus*) skin cell [35]. The observation that LiTFSI induces cell cycle arrest in S phase in HepG2 cells but not in A498 cells suggests that the effects of LiTFSI on cell cycle progression are cell type specific.

The differential regulation of cell cycle-related genes *Ccna2*, *Ccne1*, and *Ccnb1* in A498 and HepG2 cells upon exposure to LiTFSI further supports this conclusion. This finding was also confirmed in HGrC1 cells [10].

Recent studies have shown that PFAS can impair lipid metabolism and cause damage to liver lipid homeostasis in frogs [31]. Based on the experimental results, LiTFSI exposure caused significant changes in gene expression, indicating a potential impact on cellular function. The upregulation of genes involved in lipid metabolism, such as *ACSL1* and *HMGCR*, suggests a potential role in altering lipid synthesis and cholesterol levels [51]. The downregulation of genes involved in lipid catabolism, such as *ACOX2* and *ACAD11*, may indicate impaired fatty acid degradation [27]. The changes in gene expression associated with kidney injury, such as upregulation of *Harvcr1* may promote cell death [9]. Moreover, *Nfe2l2* may increase the expression of antioxidant and detoxification genes, which could protect cells from damage caused by ROS [25], consistent with the results of REDOX levels. The change in expression of *TET* and *DNMT* genes suggests that LiTFSI may influence the abundance of transcripts associated with DNA methylation [46], resulting in a significant downregulation of *DNMT3A* and *DNMT3B*. However, the effect of LiTFSI on the methylation level needs to be characterized in the future.

Overall, the results presented in this study demonstrate the short-term toxicity of LiTFSI in two different human cancer cell lines, A498 and HepG2. These findings suggest that LiTFSI, as a type of PFAS, can induce toxicity in human cells through a variety of mechanisms, including oxidative stress, apoptosis, and cell cycle dysregulation. These findings have important implications on the use of PFAS and related compounds in various applications, including consumer products and industrial processes. Future research directions could include investigating the long-term effects of LiTFSI exposure, studying the potential role of low-dose/chronic exposure to LiTFSI, and elucidating the molecular mechanisms underlying the cell type-specific effects of LiTFSI on various cellular processes.

5. Conclusions

Our work provides evidence on the short-term toxicity of LiTFSI, a novel PFAS. The results of the study showed that exposure to LiTFSI caused a decrease in cell viability and an increase in the production of ROS in both HepG2 and A498 cells. Our results are consistent with previous studies on in vitro toxicity of PFAS. Furthermore, LiTFSI was found to induce apoptosis in both the cell lines tested, and the expression of genes related to apoptosis and proliferation were affected upon exposure to LiTFSI. Additionally, LiTFSI was found to modulate cell cycle progression in a cell type-specific manner, which may have implications on therapeutic targets for cancer. These findings underscore the importance of evaluating the toxicity of emerging PFAS compounds like LiTFSI and understanding their implications for human health and the environment. Future research should focus on investigating long-term in vivo effects and elucidating molecular mechanisms underlying cell type-specific responses to LiTFSI exposure, informing risk assessment and regulatory measures.

Funding

This research was partly funded by the Campus Research Board Award# RB22002, University of Illinois at Urbana-Champaign.

CRedit authorship contribution statement

Joseph Irudayaraj: Writing – review & editing, Supervision, Project administration, Investigation, Funding acquisition, Conceptualization. **Jennifer Guelfo:** Writing – review & editing, Conceptualization. **Mindy Lin:** Methodology, Data curation. **Mia Sands:** Writing – original draft, Software, Formal analysis, Data curation. **Xing Zhang:** Writing – original draft, Validation, Methodology, Formal analysis.

Declaration of Competing Interest

The authors declare that they have no known competing financial interests or personal relationships that could have appeared to influence the work reported in this paper.

Data Availability

Data will be made available on request.

Acknowledgments

Not applicable.

Institutional Review Board Statement

“Not applicable”

Informed Consent Statement

“Not applicable.”

Appendix A. Supporting information

Supplementary data associated with this article can be found in the online version at doi:10.1016/j.toxrep.2024.02.008.

References

- [1] S. Ahmad, Y. Wen, J.M.K. Irudayaraj, PFOA induces alteration in DNA methylation regulators and SARS-CoV-2 targets Ace2 and Tmprss2 in mouse lung tissues, *Toxicol. Rep.* 8 (2021) 1892–1898.
- [2] L. Ahrens, L.W.Y. Yeung, S. Taniyasu, P.K.S. Lam, N. Yamashita, Partitioning of perfluorooctanoate (PFOA), perfluorooctane sulfonate (PFOS) and perfluorooctane sulfonamide (PFOSA) between water and sediment, *Chemosphere* 85 (2011) 731–737.
- [3] V. Amstutz, A. Cengo, F. Gehres, D. Sijm, M. Vrolijk, Investigating the cytotoxicity of per- and polyfluoroalkyl substances in HepG2 cells: a structure-activity relationship approach, *Toxicology* 480 (2022) 153312.
- [4] V.H. Amstutz, A. Cengo, F. Gehres, D.T.H.M. Sijm, M.F. Vrolijk, Investigating the cytotoxicity of per- and polyfluoroalkyl substances in HepG2 cells: a structure-activity relationship approach, *Toxicology* 480 (2022) 153312.
- [5] J. Bangma, J. Szilagy, B.E. Blake, C. Plazas, S. Kepper, S.E. Fenton, R. C. Fry, An assessment of serum-dependent impacts on intracellular accumulation and genomic response of per- and polyfluoroalkyl substances in a placental trophoblast model, *Environ. Toxicol.* 35 (2020) 1395–1405.
- [6] J. Bassler, A. Ducatman, M. Elliott, S. Wen, B. Wahlang, J. Barnett, M.C. Cave, Environmental perfluoroalkyl acid exposures are associated with liver disease characterized by apoptosis and altered serum adipocytokines, *Environ. Pollut.* 247 (2019) 1055–1063.
- [7] D.F. Calvisi, C. Wang, C. Ho, S. Ladu, S.A. Lee, S. Mattu, G. Destefanis, S. Delogu, A. Zimmermann, J. Ericsson, S. Brozzetti, T. Staniscia, X. Chen, F. Dombrowski, M. Evert, Increased lipogenesis, induced by AKT-mTORC1-RPS6 signaling, promotes development of human hepatocellular carcinoma, *Gastroenterology* 140 (2011) 1071–1083, e1075.
- [8] J. Chen, J. Lu, J. Ning, Y. Yan, S. Li, L. Zhou, Pollution characteristics, sources, and risk assessment of heavy metals and perfluorinated compounds in PM2.5 in the major industrial city of northern Xinjiang, China, *Air Qual. Atmosphere Health* (2019) 1–10.
- [9] P.Y. Cheung, P.T. Harrison, A.J. Davidson, J.A. Hollywood, In Vitro and in vivo models to study nephropathic cystinosis, *Cells* (2022).
- [10] K.L. Clark, J.W. George, G. Hua, J.S. Davis, Perfluorooctanoic acid promotes proliferation of the human granulosa cell line HGrC1 and alters expression of cell cycle genes and Hippo pathway effector YAP1, *Reprod. Toxicol.* 110 (2022) 49–59.
- [11] E. Costello, S. Rock, N. Stratakis, P. Eckel Sandrah, I. Walker Douglas, D. Valvi, D. Cserbik, T. Jenkins, A. Xanthakos Stavra, R. Kohli, S. Sisley, V. Vasilioiu, A. La Merrill Michele, H. Rosen, V. Conti David, R. McConnell, L. Chatzi, Exposure to per- and polyfluoroalkyl substances and markers of liver injury: a systematic review and meta-analysis, *Environ. Health Perspect.* 130 (2022) 046001.
- [12] K. Dale, F. Yadette, T. Horvli, X. Zhang, H.G. Frøysa, O.A. Karlsen, A. Goksoyr, Single PFAS and PFAS mixtures affect nuclear receptor- and oxidative stress-related pathways in precision-cut liver slices of Atlantic cod (*Gadus morhua*), *Sci. Total Environ.* 814 (2022) 152732.
- [13] M.G. Evich, M.J.B. Davis, J.P. McCord, B. Acrey, J.A. Awkerman, D.R.U. Knappe, A.B. Lindstrom, T.F. Speth, C. Tebes-Stevens, M.J. Strynar, Z. Wang, E.J. Weber, W. M. Henderson, J.W. Washington, Per- and polyfluoroalkyl substances in the environment, *Science* 375 (2022) eabg9065.

- [14] G. Fauconier, T. Groffen, V. Wepener, L. Bervoets, Perfluorinated compounds in the aquatic food chains of two subtropical estuaries, *Sci. Total Environ.* 719 (2020) 135047.
- [15] A. Fenner, Is PFOA a renal carcinogen? *Nat. Rev. Urol.* 17 (2020), 602–602.
- [16] A. Florentin, T. Deblonde, N. Diguio, A. Hautemaniere, P. Hartemann, Impacts of two perfluorinated compounds (PFOS and PFOA) on human hepatoma cells: cytotoxicity but no genotoxicity? *Int. J. Hyg. Environ. Health* 214 (2011) 493–499.
- [17] M. Forsthuber, A.M. Kaiser, S. Granitzer, I. Hassl, M. Hengstschläger, H. Stangl, C. Gundacker, Albumin is the major carrier protein for PFOS, PFOA, PFHxS, PFNA and PFDA in human plasma, *Environ. Int.* 137 (2020) 105324.
- [18] W.J.R. Gilbert, J. Safarov, D.L. Minnick, M.A. Rocha, E.P. Hassel, M.B. Shiflett, Density, viscosity, and vapor pressure measurements of water + lithium bis (trifluoromethylsulfonyl)imide solutions, *J. Chem. Eng. Data* 62 (2017) 2056–2066.
- [19] C. Gstalder, I. Ader, O. Cuvillier, FTY720 (Fingolimod) inhibits HIF1 and HIF2 signaling, promotes vascular remodeling, and chemosensitizes in renal cell carcinoma animal model, *Mol. Cancer Ther.* 15 (2016) 2465–2474.
- [20] M. Habibullah-Al-Mamun, M.K. Ahmed, M. Raknuzzaman, M.S. Islam, J. Negishi, S. Nakamichi, M. Sekine, M. Tokumura, S. Masunaga, Occurrence and distribution of perfluoroalkyl acids (PFAAs) in surface water and sediment of a tropical coastal area (Bay of Bengal coast, Bangladesh), *Sci. Total Environ.* 571 (2016) 1089–1104.
- [21] C.P. Higgins, J.A. Field, C.S. Criddle, R.G. Luthy, Quantitative determination of perfluorochemicals in sediments and domestic sludge, *Environ. Sci. Technol.* 39 (11) (2005) 3946–3956.
- [22] S. Hong, J.S. Khim, T. Wang, J.E. Naile, J. Park, B.-O. Kwon, S.J. Song, J. Ryu, G. Codling, P.D. Jones, Y. Lu, J.P. Giesy, Bioaccumulation characteristics of perfluoroalkyl acids (PFAAs) in coastal organisms from the west coast of South Korea, *Chemosphere* 129 (2015) 157–163.
- [23] S. Huang, P.R. Jaffé, Defluorination of Perfluorooctanoic Acid (PFOA) and Perfluorooctane Sulfonate (PFOS) by Acidimicrobium sp. Strain A6, *Environ. Sci. Technol.* 53 (2019) 11410–11419.
- [24] R.B. Jain, A. Ducatman, Associations between the concentrations of α -klotho and selected perfluoroalkyl substances in the presence of eGFR based kidney function and albuminuria: data for US adults aged 40–79 years, *Sci. Total Environ.* 838 (2022) 155994.
- [25] X. Jiang, X. Zhou, X. Yu, X. Chen, X. Hu, J. Lu, H. Zhao, Q. Cao, Y. Gu, Y. Yang, W. Jiang, M. Jin, High expression of nuclear NRF2 combined with NFE2L2 alterations predicts poor prognosis in esophageal squamous cell carcinoma patients, *Mod. Pathol.* 35 (2022) 929–937.
- [26] K. Kannan, J. Koistinen, K. Beckmen, T. Evans, J.F. Gorzelany, K.J. Hansen, P. D. Jones, E. Helle, M. Nyman, J.P. Giesy, Accumulation of perfluorooctane sulfonate in marine mammals, *Environ. Sci. Technol.* 35 (2001) 1593–1598.
- [27] S.Q. Kim, R. Mohallem, J. Franco, K.K. Buhman, K.-H. Kim, U.K. Aryal, Multi-omics approach reveals dysregulation of protein phosphorylation correlated with lipid metabolism in mouse non-alcoholic fatty liver, *Cells* (2022).
- [28] K. Kubota, K. Tamaki, T. Nohira, T. Goto, R. Hagiwara, Electrochemical properties of alkali bis(trifluoromethylsulfonyl)amides and their eutectic mixtures, *Electrochim. Acta* 55 (2010) 1113–1119.
- [29] K.H. Kucharzyk, R. Darlington, M. Benotti, R. Deeb, E. Hawley, Novel treatment technologies for PFAS compounds: a critical review, *J. Environ. Manag.* 204 (2017) 757–764.
- [30] Z. Li, Y. Zhang, F. Wang, R. Wang, S. Zhang, Z. Zhang, P. Li, J. Yao, J. Bi, J. He, M. Keerman, H. Guo, X. Zhang, M. He, Associations between serum PFOA and PFOS levels and incident chronic kidney disease risk in patients with type 2 diabetes, *Ecotoxicol. Environ. Saf.* 229 (2022) 113060.
- [31] H. Lin, Z. Liu, H. Yang, L. Lu, R. Chen, X. Zhang, Y. Zhong, H. Zhang, Per- and Polyfluoroalkyl Substances (PFASs) impair lipid metabolism in rana nigromaculata: a field investigation and laboratory study, *Environ. Sci. Technol.* 56 (2022) 13222–13232.
- [32] W. Liu, X. Zhang, Y. Wen, M.A. Anastasio, J. Irudayaraj, A machine learning approach to elucidating PFOS-induced alterations of repressive epigenetic marks in kidney cancer cells with single-cell imaging, *Environ. Adv.* 11 (2023) 100344.
- [33] Y. Lu, K. Gao, X. Li, Z. Tang, L. Xiang, H. Zhao, J. Fu, L. Wang, N. Zhu, Z. Cai, Y. Liang, Y. Wang, G. Jiang, Mass spectrometry-based metabolomics reveals occupational exposure to per- and polyfluoroalkyl substances relates to oxidative stress, fatty acid β -oxidation disorder, and kidney injury in a manufactory in China, *Environ. Sci. Technol.* 53 (2019) 9800–9809.
- [34] A.F. Ojo, Q. Xia, C. Peng, J.C. Ng, Evaluation of the individual and combined toxicity of perfluoroalkyl substances to human liver cells using biomarkers of oxidative stress, *Chemosphere* 281 (2021) 130808.
- [35] C. Otero-Sabio, M. Giacomello, C. Centellegher, F. Caicci, M. Bonato, A. Venerando, J.-M. Graic, S. Mazzariol, L. Finos, L. Corain, A. Peruffo, Cell cycle alterations due to perfluoroalkyl substances PFOS, PFOA, PFBS, PFBA and the new PFAS C6O4 on bottlenose dolphin (*Tursiops truncatus*) skin cell, *Ecotoxicol. Environ. Saf.* 244 (2022) 113980.
- [36] P. Pierozan, M. Kosnik, O. Karlsson, High-content analysis shows synergistic effects of low perfluorooctanoic acid (PFOS) and perfluorooctane sulfonic acid (PFOA) mixture concentrations on human breast epithelial cell carcinogenesis, *Environ. Int.* 172 (2023) 107746.
- [37] S. Ramesh, G.P. Ang, Impedance and FTIR studies on plasticized PMMA–LiN (CF3SO2)2 nanocomposite polymer electrolytes, *Ionics* 16 (2010) 465–473.
- [38] K. Roth, Z. Yang, M. Agarwal, W. Liu, Z. Peng, Z. Long, J. Birbeck, J. Westrick, W. Liu, M.C. Petriello, Exposure to a mixture of legacy, alternative, and replacement per- and polyfluoroalkyl substances (PFAS) results in sex-dependent modulation of cholesterol metabolism and liver injury, *Environ. Int.* 157 (2021) 106843.
- [39] P. Sen, S. Qadri, P.K. Luukkonen, O. Ragnarsdottir, A. McGlinchey, S. Jäntti, A. Juuti, J. Arola, J.J. Schlezinger, T.F. Webster, M. Orešič, H. Yki-Järvinen, T. Hyötyläinen, Exposure to environmental contaminants is associated with altered hepatic lipid metabolism in non-alcoholic fatty liver disease, *J. Hepatol.* 76 (2022) 283–293.
- [40] J.J. Shearer, C.L. Callahan, A.M. Calafat, W.-Y. Huang, R.R. Jones, V.S. Sabbisetti, N.D. Freedman, J.N. Sampson, D.T. Silverman, M.P. Purdue, J.N. Hofmann, Serum concentrations of per- and polyfluoroalkyl substances and risk of renal cell carcinoma, *JNCI: J. Natl. Cancer Inst.* 113 (2021) 580–587.
- [41] M.E. Solan, C.P. Koperski, S. Senthilkumar, R. Lavado, Short-chain per- and polyfluoroalkyl substances (PFAS) effects on oxidative stress biomarkers in human liver, kidney, muscle, and microglia cell lines, *Environ. Res.* 223 (2023) 115424.
- [42] M.-A. Verner, E. Loccisano Anne, N.-H. Morken, M. Yoon, H. Wu, R. McDougall, M. Maisonet, M. Marcus, R. Kishi, C. Miyashita, M.-H. Chen, W.-S. Hsieh, E. Andersen Melvin, J. Clewell Harvey, P. Longnecker Matthew, Associations of perfluoroalkyl substances (PFAS) with lower birth weight: an evaluation of potential confounding by glomerular filtration rate using a physiologically based pharmacokinetic model (PBPK), *Environ. Health Perspect.* 123 (2015) 1317–1324.
- [43] Z. Wang, J. Yao, H. Guo, N. Sheng, Y. Guo, J. Dai, Comparative hepatotoxicity of a novel perfluoroalkyl ether sulfonic acid, nafion byproduct 2 (h-pfmo2osa), and legacy perfluorooctane sulfonate (pfos) in adult male mice, *Environ. Sci. Technol.* 56 (2022) 10183–10192.
- [44] Y. Wen, N. Mirji, J. Irudayaraj, Epigenetic toxicity of PFOA and GenX in HepG2 cells and their role in lipid metabolism, *Toxicol. Vitr.* 65 (2020) 104797.
- [45] Y. Wen, N. Mirji, J. Irudayaraj, Epigenetic toxicity of PFOA and GenX in HepG2 cells and their role in lipid metabolism, *Toxicol. Vitr.* 65 (2020) 104797.
- [46] Y. Wen, F. Rashid, Z. Fazal, R. Singh, M.J. Spinella, J. Irudayaraj, Nephrotoxicity of perfluorooctane sulfonate (PFOS)—effect on transcription and epigenetic factors, *Environ. Epigenetics* 8 (2022) dvac010.
- [47] M. Wielsøe, M. Long, M. Ghisari, E.C. Bonefeld-Jørgensen, Perfluoroalkylated substances (PFAS) affect oxidative stress biomarkers in vitro, *Chemosphere* 129 (2015) 239–245.
- [48] L.W. Yeung, M.K. So, G. Jiang, S. Taniyasu, N. Yamashita, M. Song, Y. Wu, J. Li, J. P. Giesy, K.S. Guruge, P.K. Lam, Perfluorooctanesulfonate and related fluorochemicals in human blood samples from China, *Environ. Sci. Technol.* 40 (2006) 715–720.
- [49] S.S. Zhang, Unveiling the mystery of lithium bis (fluorosulfonyl)imide as a single salt in low-to-moderate concentration electrolytes of lithium metal and lithium-ion batteries, *J. Electrochem. Soc.* 169 (2022) 110515.
- [50] X. Zhang, J.A. Flaws, M.J. Spinella, J. Irudayaraj, The Relationship between typical environmental endocrine disruptors and kidney disease, *Toxics* 11 (2022).
- [51] C.-Z. Zhao, W. Jiang, Y.-Y. Zhu, C.-Z. Wang, W.-H. Zhong, G. Wu, J. Chen, M.-N. Zhu, Q.-L. Wu, X.-L. Du, Y.-Y. Luo, M. Li, H.-L. Wang, H. Zhao, Q.-G. Ma, G.-Y. Zhong, R.-R. Wei, Highland barley *Monascus purpureus* Went extract ameliorates high-fat, high-fructose, high-cholesterol diet induced nonalcoholic fatty liver disease by regulating lipid metabolism in golden hamsters, *J. Ethnopharmacol.* 286 (2022) 114922.